

PISCES II : 2.5-D RF Cavity Code

Yoshihisa Iwashita

Accelerator Laboratory, Nuclear Science Research Facility
Institute for Chemical Research, Kyoto University
Gokanosho, Uji, Kyoto 611, JAPAN

Abstract The RF cavity code PISCES II can evaluate all the eigenfrequencies and fields for arbitrarily shaped axially symmetric RF cavities. The solutions include symmetric ($m=0$) and asymmetric modes ($m>0$) assuming the $\sin m\theta$ and $\cos m\theta$ dependencies. Using Vector Finite Element Method, the electric or magnetic components are calculated. The resulted eigenvalue system has many zero-eigenvalue solutions, which can be filtered out by zero-filter technique from the set of solutions. The eigensolutions of the specified number are obtained simultaneously from non-zero lowest frequency.

INTRODUCTION

The original PISCES code was written in early 1980's for studying DISK-AND-WASHER (DAW) structures which have dipole modes close to the operating frequency. Because URMEL uses rectangular mesh for the calculation, the approximated boundary is different from that of the SUPERFISH, and the comparison is not straightforward. Recently some difficulties in calculating vectorial fields by Finite Element Method (FEM) have been overcome(1,2,3) and PISCES II is rewritten for studying higher order modes including dipole modes. Second order mixed-interpolation-type (linear edge and quadratic nodal) element is implemented in the version 2.40.

FORMULATION

The differential equation for electric or magnetic field to be solved are (4,5),

$$\nabla \times \nabla \times \vec{E} + k^2 \vec{E} = 0, \quad \nabla \cdot \vec{E} = 0, \quad \text{or} \quad \nabla \times \nabla \times \vec{H} + k^2 \vec{H} = 0, \quad \nabla \cdot \vec{H} = 0 \quad (\text{in } \Omega), \quad (1)$$

where $k^2 = \omega^2 \epsilon \mu$ and Ω is the entire volume. In vacuum space, $k^2 = \omega^2 / c^2$, where c is the speed of light. Boundary conditions are

$$\vec{E} \cdot \vec{n} = 0 \quad \text{or} \quad \vec{H} \cdot \vec{n} = 0 \quad \text{on magnetic boundaries } (\Gamma_m) \text{ for symmetry plane,} \quad (2)$$

$$\vec{E} \times \vec{n} = 0 \quad \text{or} \quad \vec{H} \times \vec{n} = 0 \quad \text{on electric boundaries } (\Gamma_e) \text{ for metal surfaces and} \quad (3)$$

$$\vec{E}_{left} = e^{i\phi} \vec{E}_{right} \quad \text{or} \quad \vec{H}_{left} = e^{i\phi} \vec{H}_{right} \quad \text{on periodic boundaries } (\Gamma_p), \quad (4)$$

where \vec{n} denotes the outward normal on the boundary, and ϕ is the phase advance in the problem(6,7). The periodic boundary is not a real boundary but only for a convenience of defining a problem. Because either \vec{E} or \vec{H} can be used as the field variable, only the electric field will be shown hereafter. Integrating Equ.(1) over Ω after multiplying by $\delta\vec{E}$ (virtual electric field), we get

$$\int_{\Omega} \delta\vec{E} \cdot \nabla \times \nabla \times \vec{E} dv = -k^2 \int_{\Omega} \delta\vec{E} \cdot \vec{E} dv, \quad (5)$$

and applying Green's theorem, the following relations must hold for any $\delta\vec{E}$:

$$\oint_{\Gamma} (\nabla \times \vec{E}) \times \delta\vec{E} d\vec{s} - \int_{\Omega} (\nabla \times \vec{E}) \cdot (\nabla \times \delta\vec{E}) dv = -k^2 \int_{\Omega} \delta\vec{E} \cdot \vec{E} dv \quad (6)$$

$$\vec{E} \times \vec{n} = 0 \text{ and } \delta\vec{E} \times \vec{n} = 0 \text{ on } (\Gamma_e), \text{ or } \vec{E} \cdot \vec{n} = 0 \text{ and } \delta\vec{E} \cdot \vec{n} = 0 \text{ on } (\Gamma_m) \quad (7)$$

The term in the surface integration of Equ. (6) becomes zero on either (Γ_e) or (Γ_m) because of the boundary condition of Equ's (7).

FINITE ELEMENT MODEL

Because only the axisymmetric boundary problems are considered, we can assume $\sin m\theta$ and $\cos m\theta$ dependencies of E_r , E_z and E_θ components, and then the problem can be reduced to two-dimension problem:

$$\vec{E} = (E_\theta \sin m\theta, E_r \cos m\theta, E_z \cos m\theta). \quad (8)$$

Then (E_θ, E_r, E_z) are functions of r and z only. The field variables are (rE_θ, E_r, E_z) for $m \geq 1$ and (E_θ, H_θ) for $m=0$. Only the case for $m \geq 1$ will be explained here.

The shape functions used are the mixed-interpolation-type triangular elements (3). Figure 1 shows the elements used in PISCES II. Only the tangential component in the rz -plane is assigned on the line. Either the lowest order (constant edge and linear nodal) or the second order (linear edge and quadratic nodal) element can be used. Both elements may have curved boundaries.

Then, \vec{E} and $\nabla \times \vec{E}$ can be written as

$$\vec{E} = \begin{bmatrix} E_\theta \\ E_r \\ E_z \end{bmatrix} = \vec{N} \cdot \begin{bmatrix} r\vec{E}_\theta \\ \vec{E}_{rz} \end{bmatrix}, \quad \nabla \times \vec{E} = \vec{N}' \cdot \begin{bmatrix} r\vec{E}_\theta \\ \vec{E}_{rz} \end{bmatrix}, \quad (9)$$

$$\vec{N} = \begin{bmatrix} \frac{1}{r}\vec{N}_\theta & 0 \\ 0 & \vec{N}_r \\ 0 & \vec{N}_z \end{bmatrix}, \quad \vec{N}' = \begin{bmatrix} 0 & \partial_z \vec{N}_r - \partial_r \vec{N}_z \\ \frac{-1}{r} \partial_z \vec{N}_\theta & \frac{-m}{r} \vec{N}_z \\ \frac{1}{r} \partial_r \vec{N}_\theta & \frac{m}{r} \vec{N}_r \end{bmatrix}, \quad (10)$$

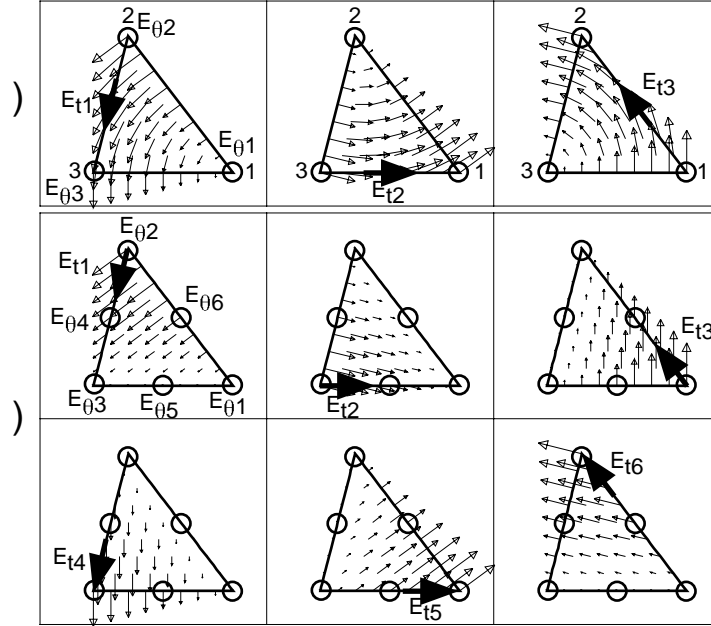


FIGURE 1. Mixed-interpolation-type triangular elements.

a) Constant edge and linear nodal elements. b) Linear edge and quadratic elements.

where \vec{N} , \vec{N}' , \vec{N}_θ , \vec{N}_z , and \vec{N}_r are the shape functions, and $r\vec{E}_\theta$ and \vec{E}_{rz} are the field variable. The element matrix equation is

$$\int_e \vec{N}'^T \cdot \vec{N}' r dr dz = -k^2 \int_e \vec{N}^T \cdot \vec{N} r dr dz, \quad (11)$$

where symbol e denotes the element volume. The integrations are performed numerically up to 11th order precision. The singularity in the integrand on the axis, is not serious because the real divergent terms are eliminated by the boundary condition on the axis. By assembling all element matrices and applying the boundary condition, finally we get the general eigenvalue equation.

$$\vec{M} \cdot \vec{x} = k^2 \vec{K} \cdot \vec{x}, \quad (14)$$

where \vec{M} and \vec{K} are large sparse symmetric matrices, and \vec{x} is an eigenvector. Usually several eigensolutions starting from the smallest one but zero are of interest. Unfortunately, this eigenvalue problem has many zero-eigenvalue solutions, and then special care should be taken, which is stated in next section.

GENERAL EIGENVALUE SOLVER FOR LARGE SPARSE SYMMETRIC MATRICES

Because the matrices are sparse, only non-zero elements are stored by list vector technique. The eigenvalue solver is based on the subspace method[8] and the zero filter technique(9). Because \vec{M} is not regular, all the eigenvalues are shifted and scaled by positive number α , and then the resulted eigenvalue equation is,

$$\vec{M}' \cdot \vec{x} = \lambda \vec{K} \cdot \vec{x}, (\vec{M}' = \vec{M}/\alpha + \vec{K}, \lambda = 1 + k^2/\alpha), \quad (15)$$

where α should be close to the lowest eigenvalue but zero. Because \vec{M}' is positive definite and symmetric, the Preconditioned Conjugate Gradient Method (PCGM) can be safely used to solve the simultaneous linear equations. The zero filter operation is expressed as

$$\vec{x}_{n+1} = \vec{x}_n - \vec{M}'^{-1} \cdot \vec{K} \cdot \vec{x}_n. \quad (16)$$

By applying this operation in the subspace iterations with the appropriate frequency, the zero-eigenvalue solutions are well suppressed from the iterated vectors. This technique is also used to accelerate the convergence of the subspace method, by filtering the higher eigenvalue solutions.

COMPONENTS OF PISCES II

Three stages are required for PISCES II calculation, namely, preprocessor, field solver and post processor. The preprocessor prepares the mesh data for the field solver PISCES II. The mesh data can be read from TAPE35 file of POISSON / SUPERFISH Rel. 4 (PS4) (10). MESHNET reads TAPE35 from LATTICE and writes out an input file for PISCES II. NETREF can modify the input file to subdivide or modify the mesh at any place. Unlike the PS4, PISCES II can handle topologically non-uniform triangular mesh, because of the Finite Element Method. The mesh generator NET is planned to generate the mesh data directly from the input data for AUTOMESH. The post processor DISPLAY displays the graphical informations of the field interactively.

EXAMPLES

The relative frequency error of the second lowest mode in the spherical cavity with a 10 cm radius as a function of the number of unknowns is shown in Fig. 2. The mode corresponds to the first mode among the dipole solutions ($m=1$) in PISCES II calculation. The reference frequency is obtained analytically. The frequency of the spherical cavity converges within 8.6×10^{-6} at the mesh size of 0.125 cm, which corresponds to 11564 elements or 58120 unknown variables. While the curved boundary capability in the lowest order element is not remarkable on the accuracy, it improves the accuracy of the second order element case. Although the relative error for the second order element is smaller than that for the lowest order element, the convergence rate does not have much difference, which was not expected for such higher order elements. It is under investigation,.

Figure 3 shows the graphical output from DISPLAY at the mesh size of 1cm, which corresponds to 973 unknown variables. The contour plot of rH_θ , arrow plot in the r-z plane and the mesh plot are shown.

Figure 4 shows the field plots of the dipole modes in a Disk-and-Washer structure. The mesh is generated by AUTOMESH/LATTICE and converted by MESHNET. The mesh around the nose is modified by NETREF to be compatible with the curved boundaries.

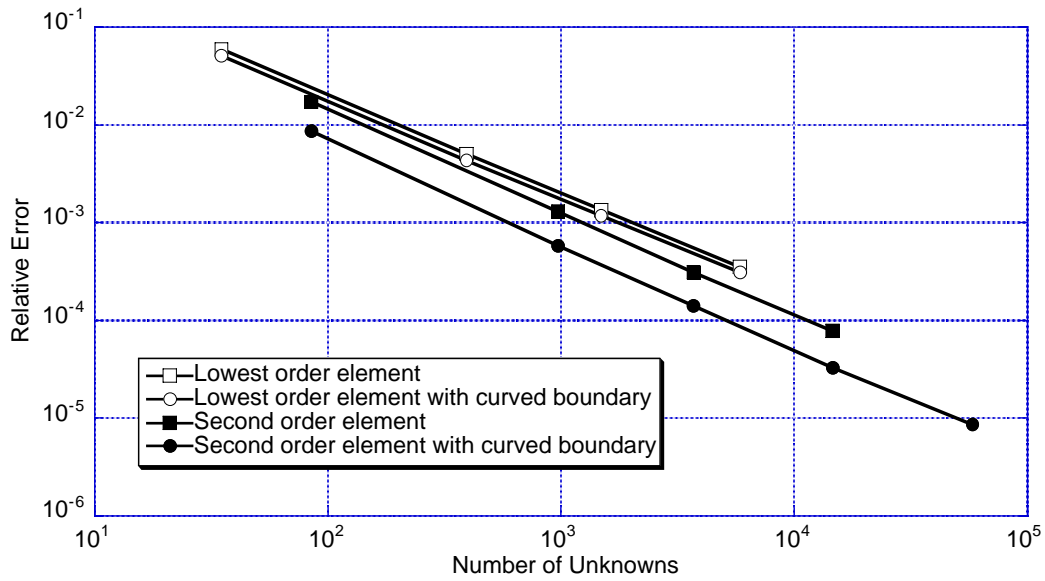


FIGURE 2 Relative frequency errors of the second lowest mode in a spherical cavity as a function of the number of unknowns.

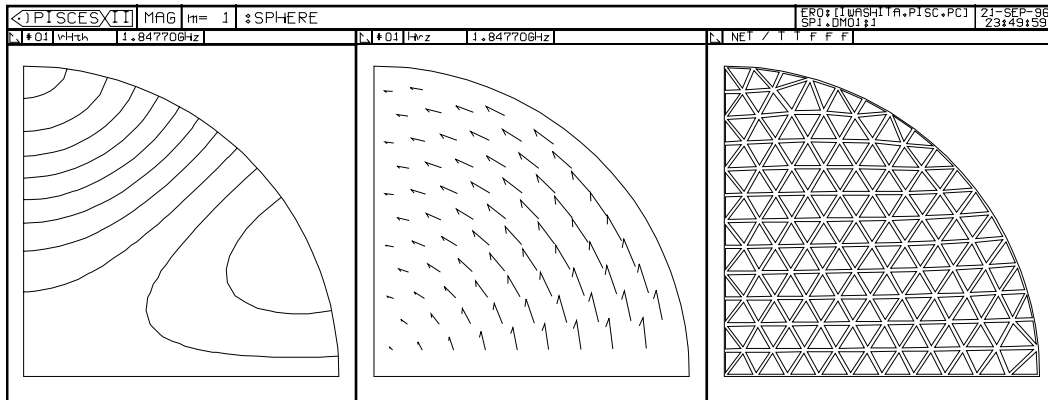


FIGURE 3. Right to left: contour plot of rH_θ , arrow plot in $r-z$ plane and mesh plot.

CONCLUSION

Any mode in a cylindrically symmetric cavity can be calculated by Vector Finite Element Method with the mixed-interpolation-type element using 2.5D approach. The convergence problem on the high order elements is under investigation.

ACKNOWLEDGEMENTS

The author would like to thank Drs. R. K. Cooper, R. L. Gluckstern, R. A. Jameson, T. Weiland and T. Higo for their encouragement and discussions. He also is greatly indebted to Dr. Maruyama for his helpful information.

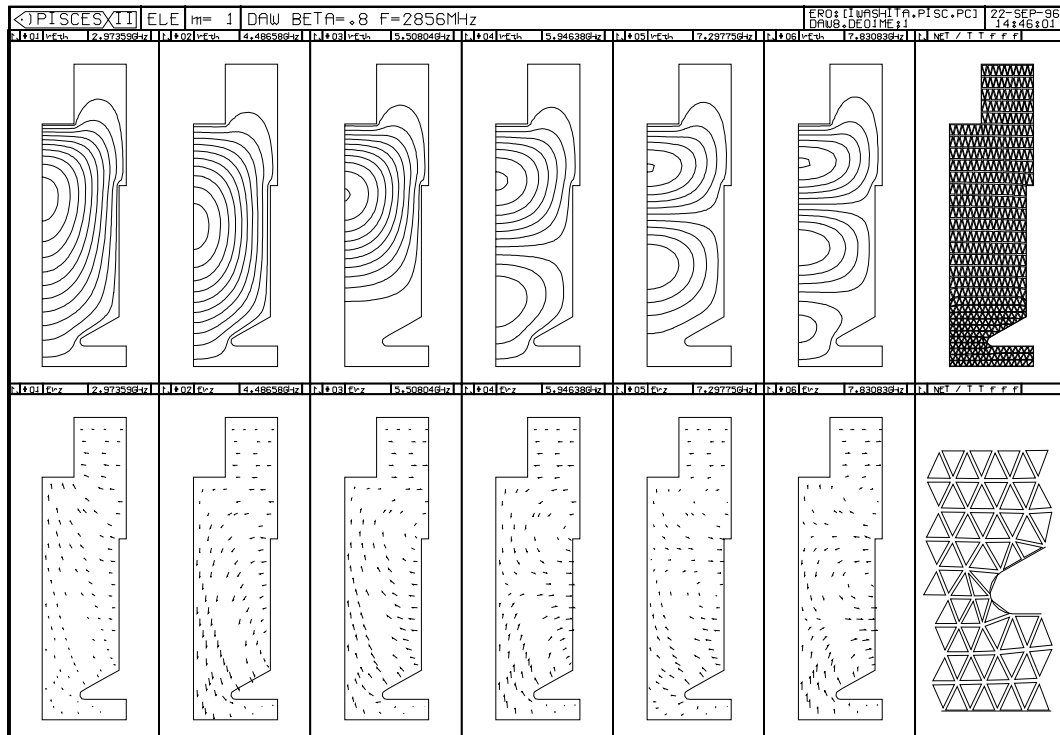


FIGURE 4. Field plots of the dipole modes in Disk-and-Washer structure. The mesh is generated by AUTOMESH/LATTICE and converted by MESHNET. The mesh around the nose is modified by NETREF to be compatible with the curved boundaries.

REFERENCES

1. F. Kikuchi, et.al., "A FINITE ELEMENT METHOD FOR 3-D ANALYSIS OF CAVITY RESONATORS", Distributed Parameter Systems: Modeling and Simulation, Elsevier Science Publishers B.V. (North-Holland) ©IMACS, 1989
2. J. C. Nédélec, "A New family of Mixed Finite Elements in R³", Num. Math., Vol. 50 pp. 57-81, 1986
3. M. Koshiba, S. Maruyama and K. Hirayama, "A Vector Finite Element Method With the High-Order Mixed-Interpolation-Type Triangular Elements for Optical Waveguiding Problems", Journal of Lightwave Technology, Vol.12, No.3, March 1994, pp.495-502.
4. M. Hara, T. Wada, T. Fukasawa, and F. Kikuchi, "A three Dimensional Analysis of RF Electro-magnetic Fields by Finite Element Method", IEEE Trans., MAG-19 No. 6 Nov. 1983
5. K. H. Huebner and E. A. Thornton, "The Finite Element Method for Engineers", (J. Wiley, New York); and A.R. Mitchell and R. Wait, "The Finite Element Method in Partial Differential Equations" (J. Wiley, New York, 1977);
6. R. L. Gluckstern and E. N. Opp, "Calculation of dispersion curves in periodic structures", IEEE Trans. MAG-21 No. 6 Nov. 85 pp. 2344-2346
7. E. M. Nelson, "A Finite Element Field Solver for Dipole Modes", 1992 Linear Accelerator Conference Proceedings, AECL, p.814
8. K.J. Bathe, "Solution Methods for Large Generalized Eigenvalue Problem in Structural Engineering", Doctoral thesis, University of California, Berkeley, 1971
9. Y. Iwashita, "General Eigenvalue Solver for Large Sparse Symmetric Matrix with Zero Filtering", Bull. Inst. Chem. Res. Kyoto Univ. Vol. 67, No. (1989)
10. "User's Guide for the POISSON/SUPERFISH Group of Codes", LA-UR-87-115, Los Alamos National Lab.